Effects of Molecular Weight on Electroluminescence of Nanogold-Bonded poly(9,9-dioctylfluorene-*alt*-thiophene) at a Constant Polymer-to-Gold Weight Ratio

Hong-Da Ji,[1] Yen-Ching Tu,[1] Sheng-Han Wu,[1] Cheng-Hao Liu,[1] Yu-Wei Su,[1] Raymond Chien-Chao Tsiang[1,2]

[1]*Department of Chemical Engineering, National Chung Cheng University, Taiwan, Republic of China*
[2]*Institute of Opto-Mechatronics, National Chung Cheng University, Chiayi 621, Taiwan, Republic of China*

Received 25 August 2008; accepted 17 March 2009
DOI 10.1002/app.30474
Published online 27 May 2009 in Wiley InterScience (www.interscience.wiley.com).

ABSTRACT: The effects of molecular weight on electroluminescent properties of the light emitting polymeric nanocomposite, poly(9,9-dioctylfluorene-*alt*-thiophene) with chemically bonded gold nanoparticles (PDOFT-Au), have been studied under a condition of constant polymer-to-gold weight ratio. The polymer, PDOFT, was first synthesized via the Suzuki cross-coupling reaction and then bonded to *in situ*-formed gold nanoparticles (AuNPs) via terminal thiol functional groups which had been generated during the quenching of polymerization. A series of PDOFT-Au's of various molecular weights have thus been synthesized. At a constant polymer-to-gold weight ratio, the average size of gold nanoparticles (AuNPs) increased with an increase in the molecular weight of PDOFT. Although an increased molecular weight led to a red shift in UV-absorption and PL spectra as well as an increased PL quantum efficiencies (Φ_{PL}) for all samples (both PDOFT and PDOFT-Au), the effect of AuNPs bonding became more noticeable when the molecular weight was higher. As for light emitting diode (LED) device fabrication, an increase in the molecular weight of PDOFT also led to a red shift in the EL spectra of the fabricated LED devices. Nevertheless, PDOFT-Au, compared with PDOFT, had a lower threshold voltage, an increased brightness and current density, and an improved photometric efficiency. Moreover, the photometric efficiency increased with an increase in the molecular weight of the polymer, from 0.298 cd/A for PDOFT-Au3 up to 0.645 cd/A for PDOFT-Au1. © 2009 Wiley Periodicals, Inc. J Appl Polym Sci 113: 3972–3979, 2009

Key words: conjugated polymer; gold nanoparticle; electroluminescence; conjugation length

INTRODUCTION

Conjugated polymeric light-emitting diodes (PLEDs) polymers have been widely studied for the applications in display devices, transistors, and sensors during the last decade. A significant amount of effort was devoted in recent years on developing novel PLED polymers with better properties such as color of the light, quantum efficiency, threshold voltage, stability, and the manufacturing process.

Among various PLED polymers, polyfluorene (PF) has gained great attention. However, despite its high photoluminescence (PL) properties and device efficiency,[1–4] PF suffers from a decrease of fluorescence in their solid-state owing to the molecular aggregation and/or the excimer formation.[5–7] Therefore, PF has often been blended/copolymerized with aryl species such as thiophene to enhance the spectral stability and electroluminescence (EL) efficiency.[8–16] Furthermore, it has been found that doping with oxide nanoparticles or metal nanoparticles[17–20] significantly suppresses the photo-oxidation of PLED polymers because of the quenching of triplet excitons which otherwise form singlet oxygen via energy transfer and cause chain scission and some carbonyl defects.[21–23]

We have reported earlier, the preliminary synthesis of poly(9,9-dioctylfluorene-*alt*-thiophene) copolymer (PDOFT) and its chemical bonding with *in situ* reduced gold nanoparticles (AuNPs).[24] The excitation of PDOFT was virtually unaffected by the bonding of AuNPs and the resulting material (PDOFT-Au) was found to have much better optoelectrical properties than a corresponding blend of PDOFT and AuNPs.[24] The PL quantum efficiencies (Φ_{PL}) for PDOFT-Au was the double of that for PDOFT and the EL of the PDOFT-Au device was nearly 10 times higher than that of the PDOFT device. These improvements prompted us to further optimize the molecular structure of PDOFT-Au. Therefore, in the current study a series of PDOFT-Au(s) of various molecular weights have been synthesized, so as to enable us to study the effects of the conjugation

Correspondence to: R. C.-C. Tsiang (chmcct@ccu.edu.tw).

length on the aggregation of AuNPs and the electroluminescent properties of PLED devices.

EXPERIMENTAL

Measurements

Gel permeation chromatography (GPC) analysis was conducted with a Waters Millennium 2010 chromatography system equipped with column sets HR0.5, HR3, HR4, and HR5E using THF as the eluent and polystyrenes as the calibration standards. The TGA 2050 system (TA Instruments, USA) was used for thermogravimetric analysis at a heating rate of 10°C/min to 800°C under nitrogen with a flow rate of 90 mL/min. A modulated DSC2910 (TA Instruments, USA) was used for differential scanning calorimeter analysis under nitrogen with a flow rate of 80 mL/min. Proton decoupled ^{1}H-NMR and ^{13}C-NMR spectra were obtained from the Varian-Unity INOVA-500 NMR (500 MHz) spectrometer with chloroform-d as the solvent and tetramethyl silane as an internal standard. The VG Scientific ESCALAB 250 with an Al Kα X-ray source (1486.6 eV) with a chamber pressure of approximately 6×10^{-10} torr provided the X-ray photoelectron spectroscopic (XPS) data. The micrographs of transmission electron microscope (TEM) were collected from High-Resolution TEM JEOL JEM-2010 at 200 kV. UV-visible and PL spectra were acquired by the HP-8453 UV-visible system and the Hitachi F-4500 with a xenon lamp, respectively. The relative quantum yields were determined using quinine sulfate in sulfuric acid as the standard ($\Phi_{PL} = 0.55$).[25] Current density-voltage (J-V) and luminescence-voltage (L-V) characteristics were measured with the Keithley 2400 high-current source measurement unit and the BN7 TOPCOM luminescence detector. The Ocean S2000 fiber optical spectrometer provided the EL spectra of the devices. All measurements were conducted under ambient conditions.

Device fabrication and characterization

Samples were prepared as a 0.75 wt % solution in THF and filtered with 0.45 μm Millex-HN filters (Millipore Co., Billerica, MA). The double-layered LED device was fabricated via a spin-coating of copolymer solution (100 nm film thickness) and poly 3,4-ethylenedioxy thiophene : poly styrenesulphonic acid (PEDOT : PSS) (30 nm film thickness) layers onto commercially available indium tin oxide (ITO) glass substrates which had undergone UV/ozone (254 nm) treatments beforehand. In the device configuration, ITO/PEDOT : PSS/copolymer/Ca/Al, the PEDOT : PSS film served as a buffer layer between the sample film and ITO substrates. The films were dried in a vacuum oven at 40°C for 5 h. Afterward, calcium (50 nm) and aluminum (100 nm) were evaporated onto the film as the cathode of the device.

Materials

Reagents were purchased from Aldrich Chemical Co. and used without further purification. Toluene was distilled over sodium before the use. Tetrahydrofuran (THF) was distilled over sodium and benzophenone.

Preparation of PDOFT-bis-4-thiol (PDOFT-SH) (example: PDOFT-SH1)

A total of 1.05 g (2.2 mmol) of 9,9-dioctylfluorene-2,7-diboronic acid (1) and 0.484 g (2 mmol) of 2,5-dibromothiophene (2) were dissolved into 20 mL of anhydrous toluene in a two-necked flask, followed by the addition of 24 mL of aqueous Na_2CO_3 (2*M*) and 0.092 g (0.23 mmol) of the phase transfer catalyst Aliquat 336. A total of 0.023 g (0.022 mmol) of tetrakis-(triphenylphosphine)palladium(0) dissolved in 10 mL of anhydrous toluene (The use of anhydrous toluene was to minimize the oxidation reaction of the catalyst) was prepared in the dry box and then transfered into the mixture mentioned above. The reaction mixture was purged under nitrogen and refluxed with vigorous stirring at 100°C for 60 h. An excessive amount of end-capper (4-bromothiophenol, 0.076 g, 0.4 mmol) was first dissolved in 1 mL anhydrous toluene and then added into the mixture. After a 12 hr reaction under stirring, the mixture was cooled to room temperature. The organic phase was washed with deionized water twice (to remove the metallic catalyst) and added into the mixture of 400 mL of methanol and 20 mL of 1*N* aqueous HCl. PDOFT-SH precipitates were collected by filtration. After a purification with Soxhlet apparatus for 3 days with methanol as the eluent, the polymeric product was reprecipitated three times and dried under vacuum at 40°C to afford a yield of 91%. Other samples, PDOFT-SH2 and PDOFT-SH3, were synthesized using the same process (yields: 81% and 50%, respectively), except for adjusting the stoichiometric imbalance of bifunctional monomers. ^{1}H-NMR ($CDCl_3$, 500 MHz, δ/ppm): δ7.784–7.394 (m, $6H_a \sim H_c$, phenyl rings of fluorene), 7.329–7.282(m, $4H_h$, thiophenol), 7.092(s, $2H_g$, thiophene), 3.475(s, $1H_i$, thiol), 2.049(s, $4H_d$, β-CH_2 of 9,9-dioctylfluorene), 1.077(s, $24H_e$, CH_2 [exclusive of β-CH_2] of 9,9-dioctylfluorene), 0.781(s, $6H_f$, CH_3 of 9,9-dioctylfluorene). Various protons are shown in Scheme 1. ^{13}C-NMR ($CDCl_3$, 125 MHz, δ/ppm): δ151.78, 144.13, 140.29, 133.28, 131.3, 128.77, 128.63, 127.19, 124.65,

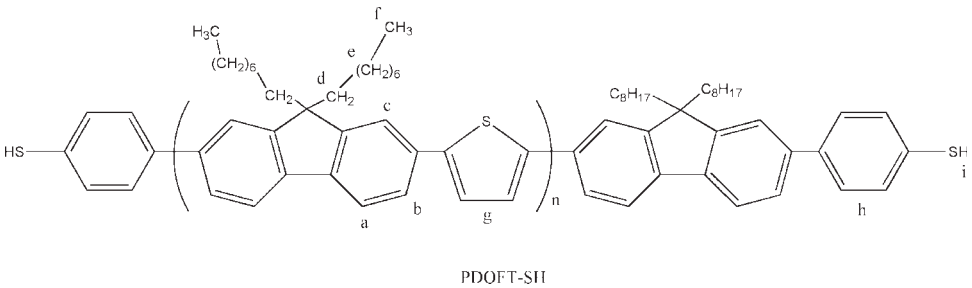

Scheme 1 Various protons in PDOFT-SH.

123.91, 122.89, 121.41, 120.13, 119.84, 55.36, 40.16, 31.78, 30.89, 30.01, 29.29, 23.78, 22.58, 14.04.

In situ formation and bonding of AuNP(s) to form PDOFT-Au

A total of 100 mg (0.254 mmol) of hydrogen tetrachloroaurate(III) hydrate ($HAuCl_4$) was dissolved in 10 mL of anhydrous THF in the dry box and then transferred into a two-necked flask which contains 300 mg of PDOFT-SH dissolved in 50 mL anhydrous THF. The reaction mixture was vigorously stirred for 60 min at room temperature before the dropwise addition of 1.0 mL lithium triethylborohydride in THF (1*M*). The color changed immediately from yellow to blackish green. The reductant was added slowly until no more gas evolved. After stirring for 2 hr at room temperature under nitrogen, the mixture was poured into centrifuge tubes filled with 20 mL absolute ethanol. PDOFT-Au precipitated and

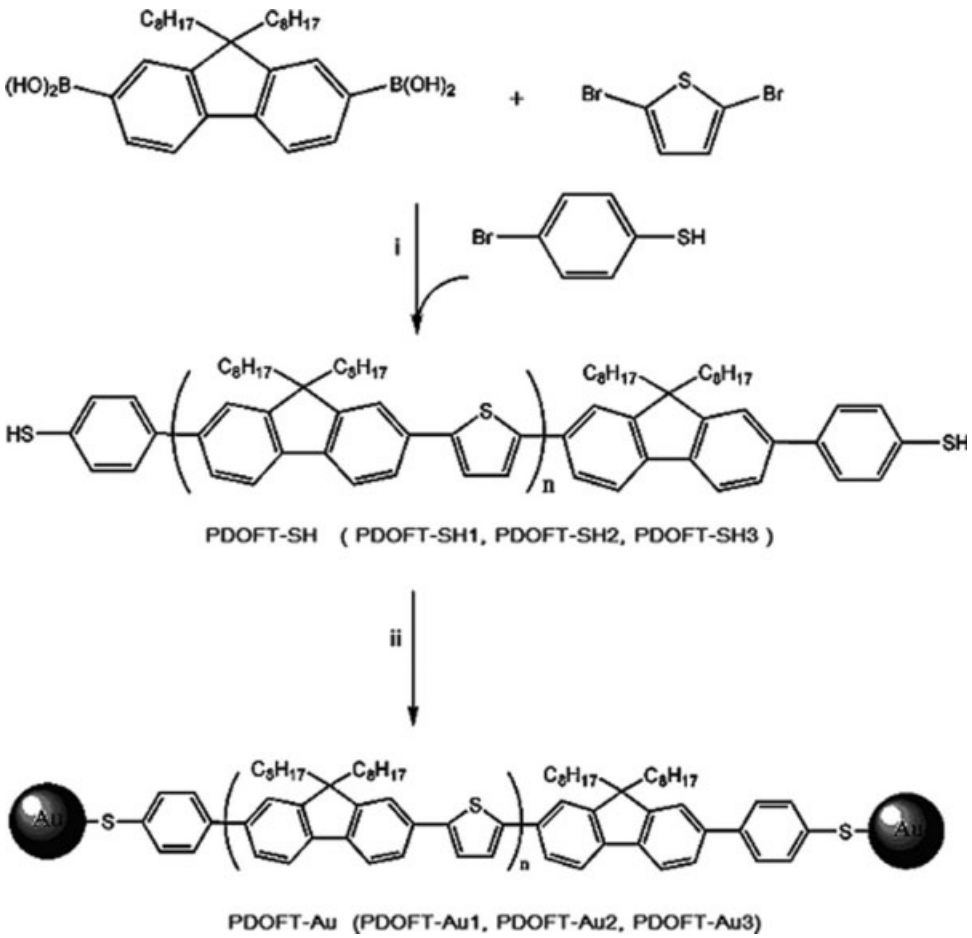

Scheme 2 Synthesis route to copolymers and polymer-functionalized gold nanoparticles. Reagents and conditions: (i) Tetrakis(triphenylphosphine) palladium (0), Aliquat 336, anhydrous toluene/Na_2CO_3 (2*M* in H_2O), reflux, 100°C; (ii) $HAuCl_4$, lithium triethylborohydride, anhydrous THF, room temperature.

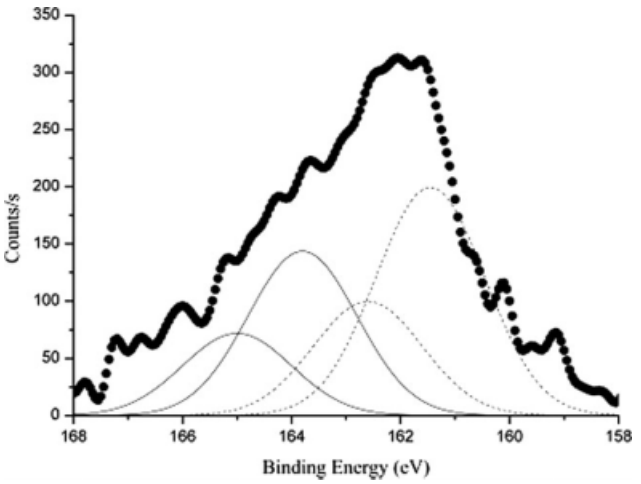

Figure 1 XPS of the sulfur 2p regions of PDOFT-SH1 bonded on Au surfaces. The solid lines show the set of sulfur doublet peaks, $S_{2p1/2}$ and $S_{2p3/2}$ and the dash lines show the set of sulfur doublet peaks, $S'_{2p1/2}$ and $S'_{2p3/2}$. The dark line shows the smoothed data.

collected. The dissolution and precipitation processes was repeated for three times in chloroform and ethanol respectively and the precipitate was purified by Soxhlet apparatus for 3 days with methanol (or acetone) as the eluent. The product was dried under vacuum at 40°C to afford blackish-green lumps. Thus, PDOFT-Au1, PDOFT-Au2, and PDOFT-Au3 samples were synthesized from PDOFT-SH1, PDOFT-SH2 and PDOFT-SH3, respectively. Yield (based on the total weight of PDOFT-SH and $HAuCl_4$): 83% (PDOFT-Au1), 80% (PDOFT-Au2), and 59% (PDOFT-Au3).

RESULTS AND DISCUSSION

Synthesis and characterization

Shown in Scheme 2 are the chemical structures and the synthesis procedures of polymers PDOFT-SH and PDOFT-Au. PDOFT-SH is formed via Suzuki coupling reaction, which couples the organoboron compound and the organic halide to create the adjacent fluorene-thiophene structure, followed by end-capping with 4-bromothiophenol. Various molecular weights of PDOFT-SH(s) were achieved by adjusting the stoichiometric imbalance of 9,9-dioctylfluorene-2,7-diboronic acid and 2,5-dibromothiophene during the polymerization, and three PDOFT-SH(s) (PDOFT-SH1, -SH2, and -SH3) have thus been synthesized. The thiol groups on these PDOFT-SH(s) were then chemically absorbed to the AuNPs, which were produced *in situ* by a reduction of hydrogen tetrachloroaurate(III) hydrate ($HAuCl_4$) with 1.0*M* lithium triethylborohydride in THF, to form PDOFT-Au(s).[9] The resulting polymers PDOFT-Au1, -Au2, and -Au3 were then purified in a Soxhlet extractor for 3 days with methanol or acetone as the eluent. The typical yield was 83% yield and the purified PDOFT-Au appeared as blackish-green lumps. All copolymers dissolved easily in common organic solvents, such as THF and chloroform, under the ambient temperature. The good solubility of copolymers resulted from the dioctyl side chains of 9,9-dioctylfluorene. The molecular structures of all copolymers were verified using ^{1}H NMR as well as ^{13}C-NMR, and the detailed data are listed in the Experimental Section. For investigating the binding between PDOFT-SH and AuNPs, XPS was used for detecting the binding energies of bound and unbound sulfur species in PDOFT-Au. Taking the S_{2p} spectrum of PDOFT-Au1 as an example (shown in Fig. 1), the anchored PDOFT-SH1 exhibited two sets of doublet peaks, S [$S_{2p1/2}$ and $S_{2p3/2}$] and S′ [$S'_{2p1/2}$ and $S'_{2p3/2}$]. The two peaks in each set were fitted with a spin–orbit splitting of 1.2 eV and an underneath area ratio of 1/2, which were in accord with results determined theoretically from spin-orbit splitting effect.[26–29] These two sets of peaks, S and S′, corroborated the presence of two types of sulfur species.

TABLE I
Characteristics of Samples

Copolymer	Fluorene : Thiophene (feed molar ratio)	Yield (%)	$M_w \times 10^3$	M_w/M_n (PDI)	T_g [°C]	T_d [°C]
PDOFT-SH1	51 : 49	91	25.8	2.96	–	424
PDOFT-SH2	57 : 43	81	14.6	2.17	–	423
PDOFT-SH3	67 : 33	50	6.8	1.45	–	407
PDOFT-Au1	51 : 49	83	25.8	2.96	–	415
PDOFT-Au2	57 : 43	80	14.6	2.17	–	406
PDOFT-Au3	67 : 33	59	6.8	1.45	–	404

M_w weight average molecular weight.
M_n number average molecular weight.
The molecular weights of PDOFT-Au(s) were not measured but were assumed to be equal to those of PDOFT-SH(s). However, one gold nanoparticle may bind two or even more PDOFT-SH molecules.

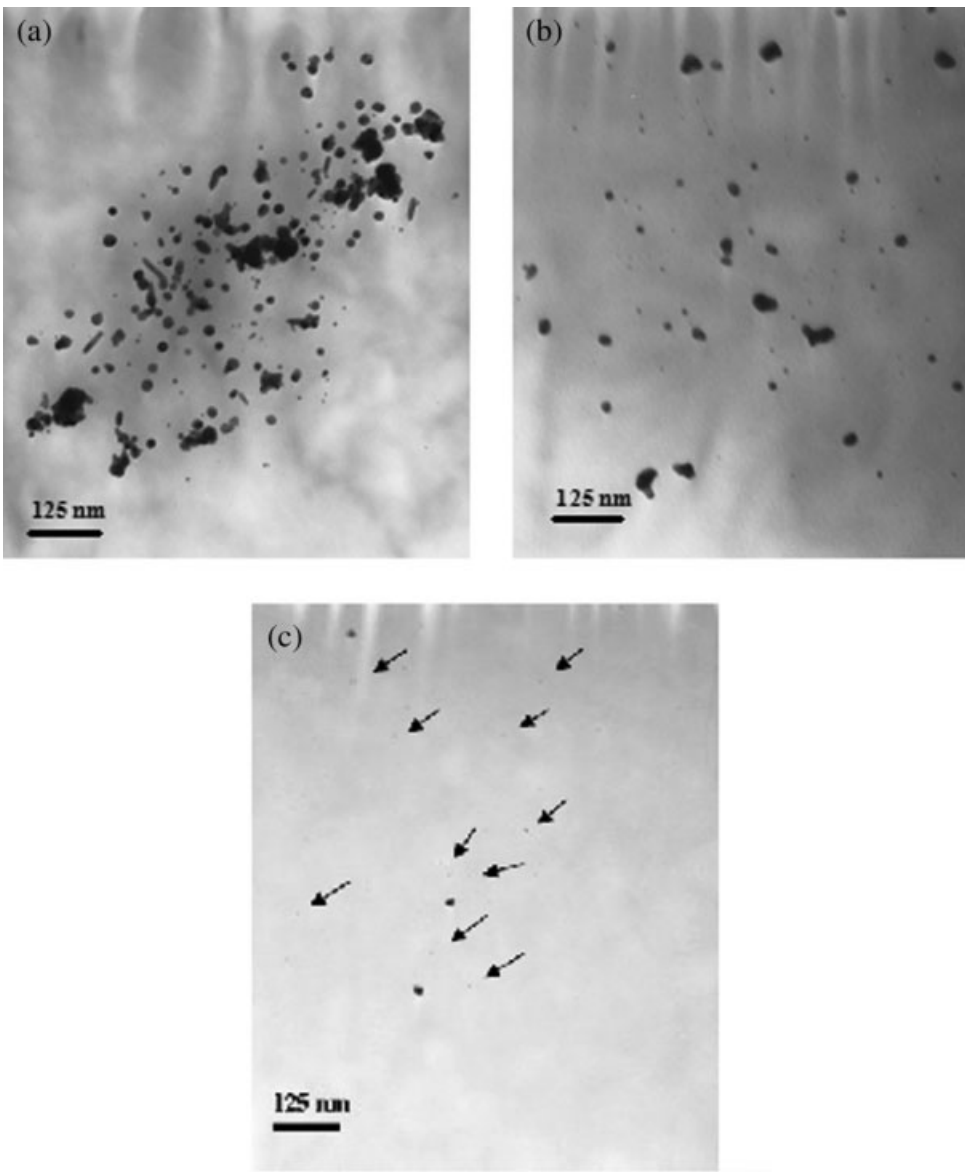

Figure 2 TEM images of the copolymers: (a) PDOFT-Au1, (b) PDOFT-Au2, and (c) PDOFT-Au3.

The peak $S_{2p3/2}$ with a binding energy of 163.8 eV corresponded to the unbound sulfur species, and the peak $S'_{2p3/2}$ with a binding energy of 161.4 eV corresponded to the sulfur bound to the gold surface. The XPS spectrum therefore served as a direct evidence for the bonding of PDOFT-SH and AuNPs.[30] Based on the underneath areas of $S_{2p3/2}$ and $S'_{2p3/2}$, the fraction of thiol-containing PDOFT bonded with AnNPs approximated to 58%.

The molecular weight M_w of each polymer (shown in Table I) was determined by the GPC with polystyrene as the calibration standard. The M_w of PDOFT-SH1PDOFT-SH3 were about 25,800–6800 g/mole, and the molecular weight distribution (PDI) were 2.96–1.45. The thermal decomposition temperatures (T_d) at a 5% weight loss were between 424 and 407°C. It was conceivable that the thermal stability of these copolymers was attributed to their rigid molecular structure. However, upon the bonding of AuNPs, T_d's were reduced to 415–404°C. This

TABLE II
UV-Vis Properties of Samples

Copolymer	UV/Vis λ_{max} (nm)		$E_g^{Optical}$(eV)[a]
	Solution	Film	
PDOFT-SH1	431	437	2.50
PDOFT-SH2	426	431	2.52
PDOFT-SH3	417	423	2.55
PDOFT-Au1	432	437	2.50
PDOFT-Au2	428	433	2.52
PDOFT-Au3	420	423	2.54

[a] Determined from the solid film onset absorption of the UV/Vis spectrum.

TABLE III
PL Properties of Samples

Copolymer	PL λ_{max} (nm) Solution[a]	PL λ_{max} (nm) Film[b]	Quantum eff. Φ_{PL}[c]	Nanoparticle effect Φ_{PL}(-Au)/Φ_{PL}(-SH)
PDOFT-SH1	475 (502)	490 (518)	0.32	–
PDOFT-SH2	472 (498)	488 (517)	0.27	–
PDOFT-SH3	468 (497)	485 (508)	0.26	–
PDOFT-Au1	473 (501)	489 (516)	0.59	1.84
PDOFT-Au2	472 (501)	489 (515)	0.41	1.52
PDOFT-Au3	468 (498)	487 (515)	0.36	1.38

[a] Values in parentheses represent the shoulder peaks.
[b] Values in parentheses represent the shoulder peaks.
[c] PL quantum efficiency were obtained by quinine sulfate in sulfuric acid as the standard ($\Phi_{reference} = 0.55$).

phenomenon was also observed previously by Walker et al. for the poly(methylphenylphosphazene)- grafted AuNPs,[31] and has been attributed to the quantum effect of AuNPs. Furthermore, T_d increases with an increase in molecular weight as expected. For all samples, the transition temperatures (T_g and T_m) were not observed, presumably because of the planar molecular configuration. To observe the dispersal and morphology of AuNPs within the film, all PDOFT-Au sample films were investigated by TEM. The effect of molecular weight of PDOFT-SH(s) on the size of formed AuNPs are illustrated by the TEM images in Figure 2(a–c) The average size of AuNPs increases with an increase in the molecular weight because of two possible reasons: (1) the -SH functional groups are insufficient to stabilize the growing AuNPs and prevent the aggregation of AuNPs; and (2) the increased interaction between copolymer chains induces more aggregation of conjugated chains.

Photophysical properties

The UV-visible absorption for all copolymers either in THF (10^{-5} mg/mL) or in a solid film are summarized in Table II. The shapes of the UV-absorption spectra do not change with the bonding of AuNPs. However, the wavelength of maximum absorption peak shows a red shift with an increase in the molecular weight of copolymers owing to the longer effective conjugation length. Based on the UV-absorption spectra of sample films, the optical ($\pi \rightarrow \pi^*$) band gaps of these samples were estimated from the onset UV-absorption wavelength according to the equation: $E_g^{OP} = \frac{hc}{\lambda}$ (where $h = 6.626 \times 10^{-34}$ Js, $c = 3.08 \times 10^8$ m/s, 1 ev $= 1.602 \times 10^{-19}$ J).

The PL emission for samples either in THF (10^{-5} mg/mL) or in a solid film are summarized in Table III. The shapes of the PL emission spectra in THF (10^{-5} mg/mL) do not change with the bonding of AuNPs, and all samples emitted bluish-green

TABLE IV
EL Properties of Samples

Copolymer	EL λ_{max} (nm)	Copolymer	EL λ_{max} (nm)
PDOFT-SH1	519	PDOFT-Au1	519
PDOFT-SH2	515	PDOFT-Au2	515
PDOFT-SH3	512	PDOFT-Au3	503

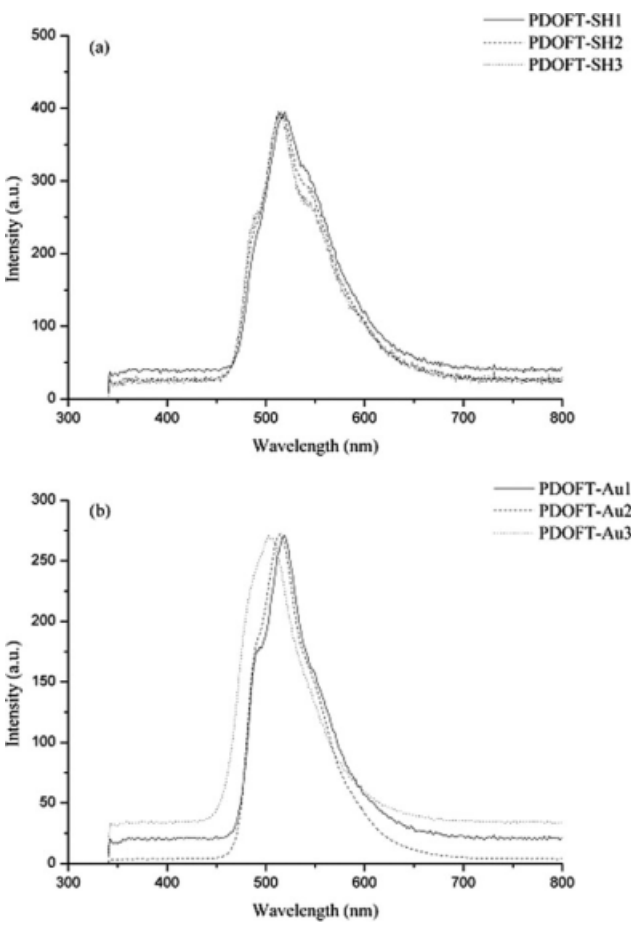

Figure 3 Room-temperature EL spectra of copolymers.

TABLE V
Characteristics of PLED Devices

Copolymer	Threshold voltage (V)	Luminescence at 9 eV (cd/m^2)	Efficiency at 9 eV (cd/A)	CIE coordinates (x, y)
PDOFT-SH1	6	1221	0.183	(0.391, 0.559)
PDOFT-SH2	6	233	0.0611	(0.331, 0.511)
PDOFT-SH3	5	423	0.0497	(0.255, 0.463)
PDOFT-Au1	3.5	6108	0.645	(0.292, 0.557)
PDOFT-Au2	4	3200	0.320	(0.299, 0.568)
PDOFT-Au3	4	3685	0.298	(0.269, 0.506)

fluorescence. The wavelength of maximum emission peak also shows a red shift with an increase in the molecular weight owing to the longer effective conjugation length in the polymer. Compared with the PL spectra in THF solution, the λ_{max}'s of all samples in a thin-film state were red-shifted and the peak became broader as a result of the chain aggregation and the extended conjugation range.[32] The measured relative PL quantum efficiencies (Φ_{PL}) are also shown in Table III, and Φ_{PL} increases with an increase in the molecular weight of samples. Nanoparticles effect could also be examined from the comparison of Φ_{PL}'s, for example, the Φ_{PL} value of PDOFT-SH1 was only 0.32, but the Φ_{PL} of PDOFT-Au1 was 0.59. Accordingly, the chemical bonding of AuNPs onto the copolymer molecule enhances the quantum efficiency significantly. The improved quantum efficiency has been attributed to the inhibitive effect on the eletron for getting into the excited triplet state.[22] Furthermore, the AuNPs effect becomes more noticeable with an increase in the molecular weight of the polymer.

El properties and current-voltage-luminance (I-V-L) characteristics of the PLED devices

Double-layered LED devices with a configuration of ITO/PEDOT : PSS/copolymer/Ca/Al were fabricated to evaluate the performances of PDOFT-SH and PDOFT-Au samples. The EL properties of all devices are summarized in Table IV, and the EL spectra are depicted in Figure 3(a,b). For every device the EL spectrum had a red shift in λ_{max} as compared with the PL spectrum of the sample in a thin-film state, and this was caused by the formation of excimers which led to energy transfer to other species.[33] Analogous to PL spectra, an increase in the molecular weight of the sample causes a little red shift in the wavelength of maximum EL peak.

The characteristics of these devices are listed in Table V. The current-voltage (I-V) relationship and the luminescence-voltage (L-V) relationship are demonstrated in Figure 4(a,b), respectively. It is noteworthy that both current density and luminescence increase when AuNPs are bonded onto the polymer molecules. This is primarily because of the enhanced interfacial contact between the polymer layer and the cathode, which enables a more efficient electron injection. The bonding of AuNPs onto the polymer also lowers the threshold voltage of the device (3.5V for PDOFT-Au1 as opposed to 6V for PDOFT-SH1). The photometric efficiency, calculated from the luminescence and the current density, of the PDOFT-Au device is nearly one order of magnitude higher than the PDOFT-SH device. Moreover, the photometric efficiency of PDOFT-Au increases with an increase in the molecular weight of PDOFT.

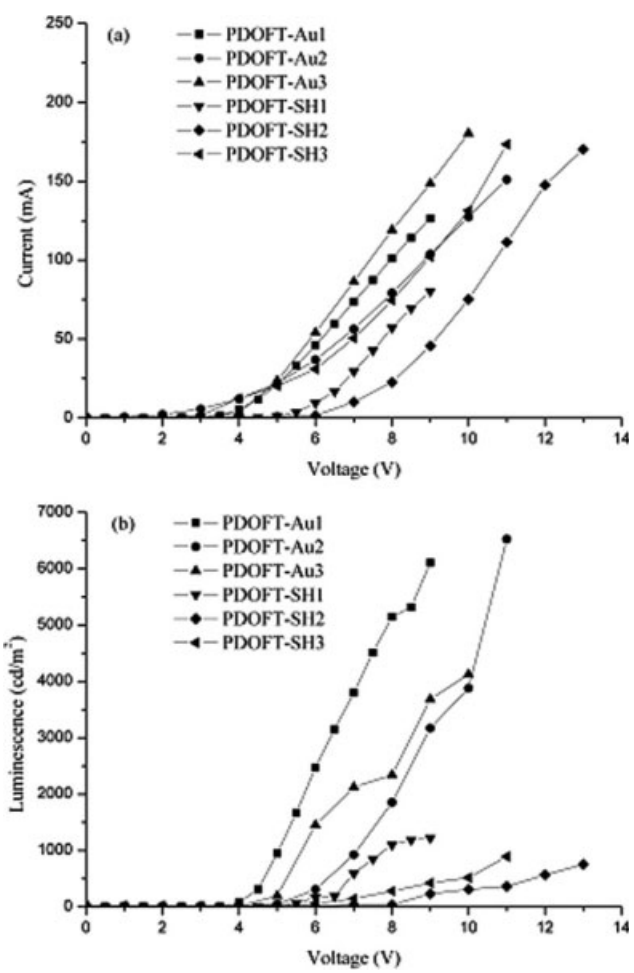

Figure 4 (a) I-V and (b) L-V characteristics of the copolymers in the double-layered devices.

CONCLUSIONS

Under a constant polymer-to-gold weight ratio, a series of PDOFT-Au's of various molecular weights have been synthesized and the various molecular weights of poly(9,9-dioctylfluorene-*alt*-thiophene) were obtained by varying the monomer feed ratios during the Suzuki cross-coupling reaction. With an increased molecular weight, the UV-absorption and PL spectra had red shifts and the average size of AuNPs and the PL quantum efficiencies (Φ_{PL}) increased. Furthermore, the AuNPs effect was more noticeable when the molecular weight was increased. For device fabrication, a higher molecular weight led to a red shift in the EL spectra, and the device fabricated with PDOFT-Au had a lowered threshold voltage, an increased brightness and current density, and an improved photometric efficiency than that fabricated with PDOFT. Furthermore, the photometric efficiency increased with an increase in the molecular weight.

Financial support provided by the National Science Council of the Republic of China under the program NSC97-2221-E-194-005 is greatly appreciated.

References

1. Pei, Q.; Yang, Y. J Am Chem Soc 1996, 188, 7416.
2. Bernius, M. T.; Inbasekaran, M.; O'brien, J.; Wu, W. Adv Mater 2000, 12, 1737.
3. Ego, C.; Grimsdale, A. C.; Uckert, F.; Yu, G.; Srdanov, G.; Müllen, K. Adv Mater 2002, 14, 809.
4. Cho, N. S.; Hwang, D. H.; Jung, B. J.; Lim, E. H.; Lee, J. M.; Shim, H. K. Macromolecules 2004, 37, 5265.
5. Grell, M.; Bradley, D. D. C.; Ungar, G.; Hill, J.; Whitehead, K. S. Macromolecules 1999, 32, 5810.
6. List, E. J. W.; Scherf, U. Adv Mater 2002, 14, 477.
7. Vamvounis, G.; Schulz, G. L.; Holdcroft, S. Macromolecules 2004, 37, 8897.
8. Klärner, G.; Davey, M. H.; Chen, W. D.; Scott, J. C.; Miller, R. D. Adv Mater 1998, 10, 993.
9. He, Y.; Gong, S.; Hattori, R.; Kanicki, J. Appl Phys Lett 1999, 74, 2265.
10. Tirapattur, S.; Belletête, M.; Drolet, N.; Leclerc, M.; Durocher, G. Chem Phys Lett 2003, 370, 799.
11. Vamvounis, G.; Holdcroft, S. Adv Mater 2004, 16, 716.
12. Yu, W. L.; Meng, H.; Pei, J.; Huang, W.; Li, Y. L. F.; Heeger, A. J. Macromolecules 1998, 31, 4838.
13. Pei, J.; Yu, W. L.; Huang, W.; Heeger, A. J. Macromolecules 2000, 33, 2462.
14. Wu, S. H.; Shen, C. H.; Chen, J. R.; Hsu, C. C.; Tsiang, R. C. C. J Polym Sci Part A: Polym Chem 2004, 42, 3954.
15. Liu, B.; Niu, Y. H.; Yu, W. L.; Cao, Y.; Huang, W. Macromolecules 2000, 33, 8945.
16. Miteva, T.; Meisel, A.; Knoll, W.; Nothofer, H. G.; Scherf, U.; Müller, D. C.; Meerholz, K.; Yasuda, A.; Neher, D. Adv Mater 2001, 13, 565.
17. Chang, W. P.; Whang, W. T. Polymer 1996, 37, 4229.
18. Carter, S. A.; Scott, J. C.; Brock, P. J Appl Phys Lett 1997, 71, 1145.
19. Hale, G. D.; Jackson, J. B.; Shmakova, J. B.; Lee, T. R.; Halas, N. J Appl Phys Lett 2001, 78, 1502.
20. Lim, Y. T.; Lee, T. W.; Lee, H. C.; Park, O. O. Synth Met 2002, 128, 133.
21. Lee, C. L.; Lee, K. B.; Kim, J. J Appl Phys Lett 2000, 77, 2280.
22. Park, J. H.; Lim, Y. T.; Park, O. O.; Kim, J. K.; Yu, J. W.; Kim, Y. C. Chem Mater 2004, 16, 688.
23. Scurlock, R. D.; Wang, B. J.; Ogilby, P. R.; Sheats, J. R.; Clough, R. L. J Am Chem Soc 1995, 117, 10194.
24. Wu, S. H.; Huang, H. M.; Chen, K. C.; Hu, C. W.; Hsu, C. C.; Tsiang, R. C. C. Adv Funct Mater 2006, 16, 1959.
25. Demas, J. N.; Crosby, G. A. J Phys Chem 1971, 75, 991.
26. Castner, D. G.; Hinds, K.; Grainger, D. W. Langmuir 1996, 12, 5083.
27. Li, Z.; Lieberman, M.; Hill, W. Langmuir 2001, 17, 4887.
28. Mayer, C. R.; Neveu, S.; Simonnet-Jégat, C.; Debiemme-Chouvy, C.; Cabuil, V.; Secheresse, F. J Mater Chem 2003, 13, 338.
29. Balasubramanian, R.; Kim, B.; Tripp, S. L.; Wang, X.; Lieberman, M.; Wei, A. Langmuir 2002, 18, 3676.
30. Zhang, H. L.; Evans, S. D.; Henderson, J. R.; Miles, R. E.; Shen, T. J Phys Chem B 2003, 107, 6087.
31. Walker, C. H.; John, J. V. S. T.; Wisian-Neilson, P. J Am Chem Soc 2001, 123, 3846.
32. Kim, J. K.; Yu, J. W.; Hong, J. M.; Cho, H. N.; Kim, D. Y.; Kim, C. Y. J Mater Chem 1999, 9, 2171.
33. Donat-Bouillud, A.; Levesque, I.; Tao, Y.; Diorio, M. Chem Mater 2000, 12, 1931.